

# Discovering overlapping communities in multi-layer directed networks

Huan Qing<sup>a,\*</sup>

<sup>a</sup>*School of Economics and Finance, Lab of Financial Risk Intelligent Early Warning and Modern Governance, Chongqing University of Technology, Chongqing, 400054, China*

---

## Abstract

This article explores the challenging problem of detecting overlapping communities in multi-layer directed networks. Our goal is to understand the underlying asymmetric overlapping community structure by analyzing the mixed memberships of nodes. We introduce a new model, the multi-layer mixed membership stochastic co-block model (multi-layer MM-ScBM), to model multi-layer directed networks in which nodes can belong to multiple communities. We develop a spectral procedure to estimate nodes' memberships in both sending and receiving patterns. Our method uses a successive projection algorithm on a few leading eigenvectors of two debiased aggregation matrices. To our knowledge, this is the first work to detect asymmetric overlapping communities in multi-layer directed networks. We demonstrate the consistent estimation properties of our method by providing per-node error rates under the multi-layer MM-ScBM framework. Our theoretical analysis reveals that increasing the overall sparsity, the number of nodes, or the number of layers can improve the accuracy of overlapping community detection. Extensive numerical experiments are conducted to validate these theoretical findings. We also apply our method to one real-world multi-layer directed network, gaining insightful results.

**Keywords:** Multi-layer directed networks, multi-layer mixed membership stochastic co-block model, overlapping community detection, spectral clustering

---

## 1. Introduction

In recent years, multi-layer networks, also known as multiplex networks, have garnered considerable attention for their ability to model complex relationships and interactions within complex systems. A multi-layer network comprises numerous interconnected networks, each layer representing a distinct type of relationship or interaction for a common set of nodes. For example, in social network analysis, nodes may represent individuals, while distinct layers might reflect friendships, familial ties, or work associations. If the relationship between any two nodes is symmetric and undirected, these multi-layer networks are classified as multi-layer undirected networks. Conversely, when the relationship is asymmetric and directed, they are known as multi-layer directed networks [1].

Community detection is a powerful tool for learning the latent community structure within networks. Its core objective is to extract community information of nodes solely based on the network's topology. For a comprehensive understanding of this technique, refer to [2, 3], which provide detailed introductions to the field of community detection. Notably, in real-world networks, a node can often be affiliated with multiple communities. In the context of directed networks, where interactions between nodes are asymmetric and directional, each node exhibits two distinct community patterns: a sending pattern and a receiving pattern. The overlapping nature of nodes, their asymmetric relationships, and the multi-layer characteristics of multi-layer directed networks further complicate community detection. We focus on the challenging problem of discovering asymmetric overlapping communities in multi-layer directed networks in this article.

A widely studied variant of this problem focuses on the scenario where the network is undirected, and each node exclusively belongs to a single community. For example, the multi-layer stochastic block model (multi-layer

---

\*Corresponding author.

Email address: [qinghuan@u.nus.edu](mailto:qinghuan@u.nus.edu) (Huan Qing)

SBM), as explored in various studies [4, 5, 6, 7], generates each layer of a multi-layer undirected network from the stochastic block model (SBM) [8], a popular statistical model for single-layer undirected networks in which communities are mutually exclusive. [4] demonstrated the estimation consistency of a spectral approach designed based on the sum of adjacency matrices, specifically under conditions where the number of layers increases while the number of nodes remains fixed, within the framework of the multi-layer SBM. [5] conducted a study on the theoretical guarantees of spectral and matrix factorization methods within the context of the multi-layer SBM. [6] introduced a least squares estimation method for communities and demonstrated its estimation consistency within the multi-layer SBM. Notably, the debiased spectral clustering algorithm introduced in [7], which offers theoretical guarantees, significantly outperforms the spectral method using the sum of adjacency matrices, the Linked Matrix Factorization method, and the Co-regularized Spectral Clustering method studied in [5]. Also see [9, 10, 11, 12] for other recent works in multi-layer undirected networks in which communities are disjoint. Unluckily, applying all algorithms above to discover communities in multi-layer directed networks is not feasible. To address this limitation, [1] proposed a spectral co-clustering algorithm that leverages the debiased approach introduced in [7] to identify disjoint communities under the multi-layer stochastic co-block model (multi-layer ScBM). This model extends the stochastic co-block model (ScBM) presented in [13] from single-layer directed networks to multi-layer directed networks. While the works in [1] address the asymmetric and directional characteristics in multi-layer directed networks, they do not extend to the general problem addressed in this article, where a node may simultaneously belong to more than one community. The key contributions of this article are as follows:

(1) We propose a flexible and interpretable statistical model, the multi-layer mixed membership stochastic co-block model (multi-layer MM-ScBM). Our model enables nodes within multi-layer directed networks to be affiliated with multiple communities.

(2) We propose a spectral method by running a vertex hunting algorithm [14] on a few leading eigenvectors of two debiased aggregation matrices to estimate nodes' mixed memberships for both the sending and receiving patterns under the multi-layer MM-ScBM framework. To our knowledge, our work is the first to discover overlapping communities in multi-layer directed networks.

(3) By deriving node-wise error bounds, we demonstrate that our method ensures consistent estimation. Our theoretical results underscore the advantages of augmenting overall sparsity, the number of nodes, or the number of layers on the problem of overlapping community detection in multi-layer directed networks. These theoretical results are verified by synthetic data, and we further illustrate the practical applications of our method by considering one real-world multi-layer directed network with encouraging results.

The structure of the remaining sections of this article is outlined in the following manner. Section 2 covers related works. Section 3 introduces the model. Section 4 presents the spectral method. Section 5 presents the consistency results. Section 6 includes both simulations and practical applications. Finally, Section 7 concludes the article. Technical proofs are in [Appendix A](#).

*Notation:* For any positive integer  $q$ , let  $[q]$  be the set  $\{1, 2, \dots, q\}$ ,  $I_{q \times q}$  be the  $q \times q$  identity matrix, and  $\|x\|_q$  be the  $l_q$  norm of vector  $x$ . For any matrix  $M$ , we use  $M'$  to denote its transpose,  $\kappa(M)$  for its condition number,  $\|M\|_F$  for the Frobenius norm,  $\text{rank}(M)$  for its rank,  $M(S, :)$  for the submatrix comprising the rows of  $M$  indexed by set  $S$ ,  $\lambda_k(M)$  for the  $k$ -th largest eigenvalue (ordered in absolute value),  $\|M\|_\infty$  for the maximum absolute row sum, and  $\|M\|_{2 \rightarrow \infty}$  for the maximum row-wise  $l_2$  norm. We further denote expectation with  $\mathbb{E}[\cdot]$  and probability with  $\mathbb{P}(\cdot)$ . Additionally, the phrase “leading  $K$  eigenvectors” refers to the eigenvectors respective to the top  $K$  eigenvalues ordered in absolute value. Lastly,  $e_i$  represents the standard basis vector that has the  $i$ -th element equal to 1, while all other elements are set to zero.

## 2. Related works

Our proposed method has a close relationship with the debiased spectral clustering methodologies presented in [7, 1]. For non-overlapping community detection in multi-layer undirected networks, [7] proposes a debiased spectral clustering algorithm by applying the K-means algorithm to several leading eigenvectors of an aggregation matrix under the multi-layer SBM model. [1] extends the idea in [7] from multi-layer undirected networks modeled by multi-layer SBM to multi-layer directed networks modeled by multi-layer ScBM. The numerical findings in [7] and [1] indicate that debiased spectral clustering achieves superior performance compared to traditional spectral clustering methods that rely on the summation of adjacency matrices or the squared summation of adjacency matrices.

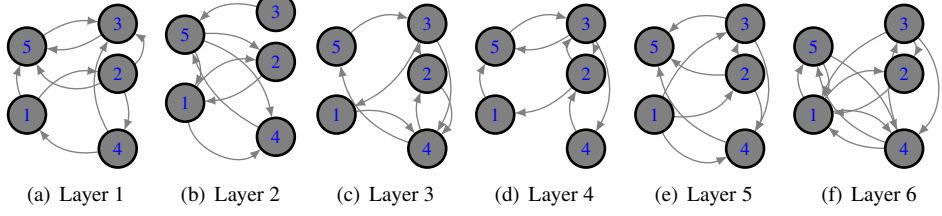


Figure 1: A toy multi-layer directed network with 5 nodes and 6 layers.

However, multi-layer ScBM can not capture the overlapping community structure of multi-layer directed networks. The mixed membership stochastic block model (MMSB) [15] allows each node to belong to multiple communities for single-layer undirected networks. The multi-way blockmodel introduced in [16] extends MMSB from undirected networks to directed networks. [17] develops an efficient spectral algorithm to estimate overlapping community memberships and derives the node-wise error bounds under MMSB. [18] develops an algorithm with theoretical guarantees to fit a degree-corrected version of MMSB. [19] designs two regularized spectral clustering algorithms based on a regularized Laplacian matrix to estimate nodes' memberships under MMSB. For works on overlapping community detection in [17, 19, 18], vertex hunting algorithms developed in [20, 14, 21, 18] are applied to hunt for pure nodes, as defined later. In this article, the proposed spectral method combines the debiased idea in [7, 1] and the vertex hunting technique in [17] to estimate nodes's mixed memberships under the proposed model.

For our theoretical analysis, we obtain the row-wise eigenspace error of two debiased aggregation matrices by using the Bernstein inequality of [22] and Theorem 4.2 of [23]. Subsequently, we employ theoretical frameworks from [17] to establish row-wise error bounds. By doing so, we broaden the scope of the theoretical analysis in [17], extending it from single-layer undirected networks to multi-layer directed networks, and from adjacency matrices to debiased aggregation matrices.

### 3. Model framework: multi-layer MM-ScBM

This article assumes that the multi-layer directed network  $\mathcal{N}$  comprises  $L$  distinct layers, each sharing a common set of  $n$  interconnected nodes. Let  $A_l \in \{0, 1\}^{n \times n}$  denote the adjacency matrix of the  $l$ -th layer directed network  $\mathcal{N}_l$ , where  $A_l(i, j) = 1$  indicates the presence of a directed edge from node  $i$  to node  $j$  (i.e.,  $i \rightarrow j$ ) and  $A_l(i, j) = 0$  otherwise, for all  $i, j \in [n]$  and  $l \in [L]$ . Therefore, in  $A_l$ , its  $i$ -th row captures the outgoing edges from node  $i$ , while its  $i$ -th column details the incoming edges to node  $i$  at the  $l$ -th layer for  $i \in [n], l \in [L]$ . Figure 1 displays a toy example of a multi-layer directed network, showcasing how nodes establish distinct connections across various layers. For the sending pattern, we assume that all nodes are classified into  $K$  distinguishable row communities:

$$C_{r,1}, C_{r,2}, \dots, C_{r,K}. \quad (1)$$

Let  $\Pi_r$  be an  $n \times K$  row membership matrix that is common to all layers. Specifically,  $\Pi_r(i, k)$  represents the “weight” indicating the affiliation of node  $i$  to the  $k$ -th row community  $C_{r,k}$  for  $i \in [n], k \in [K]$ .

Analogously, for the receiving pattern, we assume that all nodes are categorized into  $K$  column communities:

$$C_{c,1}, C_{c,2}, \dots, C_{c,K}. \quad (2)$$

Furthermore, let  $\Pi_c$  be an  $n \times K$  column membership matrix that is common across all layers and  $\Pi_c(i, k)$  represents the “weight” indicating the affiliation of node  $i$  to the  $k$ -th column community  $C_{c,k}$  for  $i \in [n], k \in [K]$ .

Because  $\Pi_r(i, :)$  is the row membership vector of node  $i$ , we have  $\|\Pi_r(i, :)\|_1 = 1$  and  $\Pi_r(i, k) \in [0, 1]$  for  $i \in [n], k \in [K]$ . Similarly, we have  $\|\Pi_c(i, :)\|_1 = 1$  and  $\Pi_c(i, k) \in [0, 1]$ .

A node  $i$  is considered “pure” in the sending pattern if  $\Pi_r(i, :)$  has exactly one entry equal to 1 and the remaining  $(K - 1)$  entries are 0. Conversely, it is deemed “mixed” if this condition does not hold for  $i \in [n]$ . A similar definition holds for nodes in the receiving pattern. For the rest of this article, we assume that  $K$  is known and

$$\text{each row and column community must contain at least one pure node.} \quad (3)$$

Without loss of generality, we rearrange the nodes' order such that  $\Pi_r(\mathcal{I}_r, :) = I_{K \times K}$  and  $\Pi_c(\mathcal{I}_c, :) = I_{K \times K}$ . Here,  $\mathcal{I}_r$  represents the indices of  $K$  pure nodes, each belonging to a distinct row community, while  $\mathcal{I}_c$  denotes the indices of  $K$  pure nodes, each from a unique column community. For each adjacency matrix  $A_l$  for  $l \in [L]$ , the model considered in this article assumes that it is generated from a directed version of MMSB. In particular, we consider the following model.

**Definition 1.** (multi-layer MM-ScBM) For  $l \in [L]$ , our multi-layer mixed membership stochastic co-block model (multi-layer MM-ScBM) generates the  $l$ -th adjacency matrix  $A_l$  in the following way:

$$\Omega_l := \rho \Pi_r B_l \Pi'_c \quad A_l(i, j) \sim \text{Bernoulli}(\Omega_l(i, j)) \quad i \in [n], j \in [n], \quad (4)$$

where  $B_l \in [0, 1]^{K \times K}$  and  $\rho \in (0, 1]$ .

In the definition of multi-layer MM-ScBM, the asymmetric matrix  $B_l$  can be different for different layers, and this guarantees that  $A_l$  may be generated from the model with common membership matrices and possibly different edge probabilities. Meanwhile, since  $\mathbb{P}(A_l(i, j) = 1) = \Omega_l(i, j) = \rho \Pi_r(i, :) B_l \Pi'_c(j, :) \leq \rho$  for  $i \in [n], j \in [n], l \in [L]$ , we observe that a reduction in the value of  $\rho$  leads to a decrease in the likelihood of an edge forming between any two nodes, thereby controlling the overall sparsity of the multi-layer bipartite network. Consequently, we refer to  $\rho$  as the sparsity parameter in this article. Given the set of  $L$  adjacency matrices  $\{A_l\}_{l=1}^L$ , our goal is to estimate  $\Pi_r$  and  $\Pi_c$  in this article. Similar to the consistency analysis conducted in [24, 17] for single-layer networks, we will permit  $\rho$  to approach zero as  $n$  and  $L$  increase in our theoretical analysis.

**Remark 1.** Our model encompasses numerous previous models as specific cases. When all nodes are pure, it simplifies to the multi-layer ScBM discussed in [1]. If the network is undirected and all nodes are pure, it reduces to the multi-layer SBM studied in [4, 5, 6, 7]. Further, for  $L = 1$ , it degenerates to the multi-way blockmodel presented in [16]. In the case of  $L = 1$  and an undirected network, it reduces to the MMSB model proposed in [15]. Moreover, when all nodes are pure and the network only has a single layer, it reduces to the ScBM model described in [13]. Finally, if the network is also undirected, it simplifies to the SBM introduced in [8].

## 4. Methodology: CSPDSoS

In this section, we introduce an efficient spectral method to estimate membership matrices  $\Pi_r$  and  $\Pi_c$  for adjacency matrices  $\{A_l\}_{l=1}^L$  generated from the multi-layer MM-ScBM by Equation (4). To explain the main idea behind our method, we provide an ideal method with knowing the  $L$  population adjacency matrices  $\{\Omega_l\}_{l=1}^L$  in Section 4.1 and modify it to the real case with observing the  $L$  adjacency matrices  $\{A_l\}_{l=1}^L$  in Section 4.2.

### 4.1. Oracle case

For the oracle case when  $\{\Omega_l\}_{l=1}^L$  are known, we define two aggregate matrices  $\tilde{S}_r$  and  $\tilde{S}_c$ :  $\tilde{S}_r = \sum_{l \in [L]} \Omega_l \Omega'_l$  and  $\tilde{S}_c = \sum_{l \in [L]} \Omega'_l \Omega_l$ . The following lemma is the starting point of our method.

**Lemma 1.** Given that the rank of  $\sum_{l \in [L]} B_l B'_l$  and  $\sum_{l \in [L]} B'_l B_l$  is  $K$ , the following conclusions can be drawn:

- Let  $U_r$  represent the leading  $K$  eigenvectors of  $\tilde{S}_r$  such that  $U'_r U_r = I_{K \times K}$ . Then, it holds that  $U_r = \Pi_r U_r(\mathcal{I}_r, :)$ .
- Similarly, let  $U_c$  represent the leading  $K$  eigenvectors of  $\tilde{S}_c$  satisfying  $U'_c U_c = I_{K \times K}$ . It follows that  $U_c = \Pi_c U_c(\mathcal{I}_c, :)$ .

The form of  $U_r = \Pi_r U_r(\mathcal{I}_r, :)$  is known as ideal simplex, where the rows of  $U_r$  locate in a simplex in  $\mathbb{R}^K$  with vertices being the  $K$  rows of  $U_r(\mathcal{I}_r, :)$ . Such ideal simplex has been observed in single layer mixed membership community detection [25, 17, 19, 18, 26], topic modeling [27, 28], and latent class analysis [29, 30]. Since  $U_r(\mathcal{I}_r, :)$  is a  $K \times K$  full rank matrix, we have  $\Pi_r = U_r U_r^{-1}(\mathcal{I}_r, :)$ , which indicates that we can exactly recover the row membership matrix through  $U_r U_r^{-1}(\mathcal{I}_r, :)$  as long as the index set  $\mathcal{I}_r$  is available. Benefited from the simplex structure  $U_r = \Pi_r U_r(\mathcal{I}_r, :)$ , applying the Successive Projection Algorithm (SPA) [20, 14, 21] to all rows of  $U_r$  with  $K$  clusters can exactly hunt for the  $K$  vertices (i.e., the  $K$  rows of  $U_r(\mathcal{I}_r, :)$ ) in the simplex. Similarly,  $U_c = \Pi_c U_c(\mathcal{I}_c, :)$  also forms an ideal simplex structure and applying the SPA to  $U_c$  can exactly recover  $\mathcal{I}_c$ . The following four-stage algorithm called ideal Co-clustering by Sequential Projection on the Debiased Sum of Squared matrices (ideal CSPDSoS) summarizes the above analysis. Input:  $\{\Omega_l\}_{l=1}^L$  and  $K$ . Output:  $\Pi_r$  and  $\Pi_c$ .

- *Aggregation step.* Set  $\tilde{S}_r = \sum_{l \in [L]} \Omega_l \Omega'_l$  and  $\tilde{S}_c = \sum_{l \in [L]} \Omega'_l \Omega_l$ .
- *Eigen decomposition step.* Obtain  $U_r$  and  $U_c$ , the leading  $K$  eigenvectors of  $\tilde{S}_r$  and  $\tilde{S}_c$ , respectively.
- *Vertex hunting step.* Run SPA to  $U_r$ 's (and  $U_c$ 's) rows with  $K$  clusters to get  $\mathcal{I}_r$  (and  $\mathcal{I}_c$ ).
- *Membership reconstruction step.* Set  $\Pi_r = U_r U_r^{-1}(\mathcal{I}_r, :)$  and  $\Pi_c = U_c U_c^{-1}(\mathcal{I}_c, :)$ .

#### 4.2. Real case

In practice, we observe the  $L$  adjacency matrices  $\{A_l\}_{l=1}^L$  instead of their expectations  $\{\Omega_l\}_{l=1}^L$ . Let  $D_l^r$  and  $D_l^c$  be two  $n \times n$  diagonal matrices such that  $D_l^r(i, i) = \sum_{j \in [n]} A_l(i, j)$  and  $D_l^c(i, i) = \sum_{j \in [n]} A_l(j, i)$  for  $i \in [n], l \in [L]$ . Define  $S_r$  and  $S_c$  as  $S_r = \sum_{l \in [L]} (A_l A_l' - D_l^r)$  and  $S_c = \sum_{l \in [L]} (A_l' A_l - D_l^c)$ . Drawing from the insightful analysis conducted in [7, 1], we know that  $S_r$  and  $S_c$  are debiased estimations of  $\tilde{S}_r$  and  $\tilde{S}_c$ , respectively. Let  $\hat{U}_r$  and  $\hat{U}_c$  be the leading  $K$  eigenvectors of  $S_r$  and  $S_c$ , respectively. We see that  $\hat{U}_r$  and  $\hat{U}_c$  can be viewed as good approximations of  $U_r$  and  $U_c$ , respectively. Then applying SPA to all rows of  $\hat{U}_r$  (and analogously to  $\hat{U}_c$ ) with  $K$  clusters should obtain accurate estimations of the index sets  $\mathcal{I}_r$  (and  $\mathcal{I}_c$ ). Algorithm 1 summarizes the above analysis.

---

#### Algorithm 1 Co-clustering by Sequential Projection on the Debiased Sum of Squared matrices (CSPDSoS)

---

**Require:**  $A_l \in \{0, 1\}^{n \times n}$  for  $l \in [L]$  and  $K$ .

**Ensure:**  $\hat{\Pi}_r$  and  $\hat{\Pi}_c$ .

- 1: Set  $S_r = \sum_{l \in [L]} (A_l A_l' - D_l^r)$  and  $S_c = \sum_{l \in [L]} (A_l' A_l - D_l^c)$ .
- 2: Obtain  $\hat{U}_r$  and  $\hat{U}_c$ , the leading  $K$  eigenvectors of  $S_r$  and  $S_c$ , respectively.
- 3: Run SPA to  $\hat{U}_r$ 's (and  $\hat{U}_c$ 's) rows with  $K$  clusters to get the estimated index set  $\hat{\mathcal{I}}_r$  (and  $\hat{\mathcal{I}}_c$ ).
- 4: Set  $\hat{Y}_r = \max(0, \hat{U}_r \hat{U}_r^{-1}(\hat{\mathcal{I}}_r, :))$  and  $\hat{Y}_c = \max(0, \hat{U}_c \hat{U}_c^{-1}(\hat{\mathcal{I}}_c, :))$ .
- 5: Set  $\hat{\Pi}_r(i, :) = \frac{\hat{Y}_r(i, :)}{\|\hat{Y}_r(i, :)\|_1}$  and  $\hat{\Pi}_c(i, :) = \frac{\hat{Y}_c(i, :)}{\|\hat{Y}_c(i, :)\|_1}$  for  $i \in [n]$ .

---

The computational cost of CSPDSoS is primarily attributed to steps 1, 2, and 3. Specifically, the time complexities of these steps are  $O(n^3L)$ ,  $O(n^3)$ , and  $O(nK^2)$ , respectively. Given that  $K \ll n$  in this article, the overall complexity of CSPDSoS is dominated by the  $O(n^3L)$  term, rendering its total complexity as  $O(n^3L)$ .

## 5. Main results

In this section, we establish per-node error bounds for the CSPDSoS algorithm's performance, demonstrating that the estimated membership matrices  $\hat{\Pi}_r$  and  $\hat{\Pi}_c$  converge closely to  $\Pi_r$  and  $\Pi_c$ , respectively. To achieve this, we introduce the following assumption to govern  $\mathcal{N}$ 's sparsity.

**Assumption 1.**  $\rho^2 n^2 L \gg \log(n + L)$ .

Assumption 1 says that the sparsity parameter  $\rho$  should diminish at a rate slower than  $\sqrt{\frac{\log(n+L)}{n^2L}}$ , aligning with the sparsity condition specified in Theorem 1 of [7]. We also assume that the smallest singular values of  $\sum_{l \in [L]} B_l B_l'$  and  $\sum_{l \in [L]} B_l' B_l$  satisfy a linear growth respective to the layers  $L$ .

**Assumption 2.** The smallest singular values of  $\sum_{l \in [L]} B_l B_l'$  and  $\sum_{l \in [L]} B_l' B_l$  are at least  $c_1 L$  and  $c_2 L$  for some constants  $c_1 > 0$  and  $c_2 > 0$ , respectively.

Analogous to Assumption 1(a) presented in [7] and the conditions outlined in Corollary 3.1 of [17], the following condition serves to facilitate our analysis.

**Condition 1.**  $K = O(1)$ ,  $\lambda_K(\Pi'_r \Pi_r) = O(\frac{n}{K})$ , and  $\lambda_K(\Pi'_c \Pi_c) = O(\frac{n}{K})$ .

The theorem presented below serves as our key theoretical contribution, offering insights into the per-node error rates of the estimated mixed memberships delivered by our CSPDSoS algorithm.

**Theorem 1.** If Assumptions 1, 2, and Condition 1 are satisfied, with probability  $1 - o(\frac{1}{n+L})$ ,

$$\max_{i \in [n]} \|e'_i(\hat{\Pi}_r - \Pi_r \mathcal{P}_r)\|_1 = O(\sqrt{\frac{\log(n+L)}{\rho^2 n^2 L}}) + O(\frac{1}{n}), \max_{i \in [n]} \|e'_i(\hat{\Pi}_c - \Pi_c \mathcal{P}_c)\|_1 = O(\sqrt{\frac{\log(n+L)}{\rho^2 n^2 L}}) + O(\frac{1}{n}),$$

where  $\mathcal{P}_r$  and  $\mathcal{P}_c$  are two  $K \times K$  permutation matrices.

According to Theorem 1, enhancing  $\rho$  or increasing  $n$  leads to more precise estimations of  $\Pi_r$  and  $\Pi_c$ . Additionally, an augmentation in the number of layers  $L$  results in a reduction in error rates, indicating that the utilization of multiple layers can significantly benefit the process of community detection.

## 6. Numerical experiments

### 6.1. Synthetic data

We first investigate CSPDSoS's performance on synthetic multi-layer directed networks by considering different values of the parameters  $n, \rho$ , and  $L$ .

*Algorithms for comparison.* While [1] proposed an efficient method for community detection in multi-layer ScBM for non-overlapping multi-layer directed networks, it is unable to estimate nodes' mixed memberships in overlapping multi-layer directed networks. Therefore, similar to [7, 1], we consider the following two approaches for comparison:

- **CSPSum:** Co-clustering by Sequential Projection on the **Sum** of adjacency matrices. This method takes the leading  $K$  left (and right) singular vectors of  $\sum_{l \in [L]} A_l$  to replace  $\hat{U}_r$  (and  $\hat{U}_c$ ) in Algorithm 1.
- **CSPSoS:** Co-clustering by Sequential Projection on the **Sum of Squared** matrices. CSPSoS takes  $\sum_{l \in [L]} A_l A'_l$  and  $\sum_{l \in [L]} A'_l A_l$  to replace  $S_r$  and  $S_c$  in Algorithm 1, respectively.

*Evaluation metrics.* Hamming Error and Relative Error serve as metrics for evaluating the performance of various methods. Hamming Error is calculated as  $\max\left(\frac{\min_{\mathcal{P} \in S} \|\hat{\Pi}_r \mathcal{P} - \Pi_r\|_1}{n}, \frac{\min_{\mathcal{P} \in S} \|\hat{\Pi}_c \mathcal{P} - \Pi_c\|_1}{n}\right)$ , where  $S$  represents the set of all  $K \times K$  permutation matrices. This metric ranges from 0 to 1, with a lower value indicating superior performance. Relative Error, on the other hand, is defined as  $\max\left(\frac{\min_{\mathcal{P} \in S} \|\hat{\Pi}_r \mathcal{P} - \Pi_r\|_F}{n}, \frac{\min_{\mathcal{P} \in S} \|\hat{\Pi}_c \mathcal{P} - \Pi_c\|_F}{n}\right)$  and is a non-negative value. The closer it is to zero, the better the performance.

*Simulation configurations.* For synthetic multi-layer directed networks, we specify  $K = 3$  and denote  $n_0^r$  and  $n_0^c$  as the respective number of pure nodes in each row and column community. For the mixed membership of a mixed node  $i$  belonging to the row community, we assign  $r_1 = \frac{\text{rand}(1)}{2}$ ,  $r_2 = \frac{\text{rand}(1)}{2}$ , and  $r_3 = 1 - r_1 - r_2$ , where  $\text{rand}(1)$  is a random value in  $[0, 1]$ . Then we set  $\Pi_r(i, :) = (r_1, r_2, r_3)$ . A similar approach is employed to generate the mixed memberships of nodes in the column community. Each entry of  $B_l$  for  $l \in [L]$  is randomly drawn from  $[0, 1]$ . For each experiment,  $n, L, \rho, n_0^r$ , and  $n_0^c$  are set independently. Finally, we report the average of each metric, obtained by conducting 100 independent repetitions under each set of configurations.

*Experiment 1.* Here, our goal is to explore how the performance of these methods evolves as the number of nodes increases. To achieve this, we set  $L = 10$ ,  $\rho = 0.02$ ,  $n_0^r = \frac{n}{4}$ ,  $n_0^c = \frac{n}{5}$ , and vary  $n$  within the set  $\{500, 1000, 1500, \dots, 5000\}$ .

*Experiment 2.* The objective of this experiment is to assess the impact of increasing the number of layers  $L$  in multi-layer directed networks on the methods' effectiveness. For this, we maintain constant values of  $n = 200, \rho = 0.1, n_0^r = 50, n_0^c = 40$ , while varying  $L$  from the set  $\{10, 20, 30, \dots, 100\}$ .

*Experiment 3.* In this experiment, we seek to investigate the influence of the overall sparsity  $\rho$  on the performance of the methods. We keep  $n = 500, L = 20, n_0^r = 80, n_0^c = 120$  fixed, and test various values of  $\rho$  from the range  $\{0.05, 0.1, 0.15, \dots, 0.5\}$ .

*Results.* By Figure 2, we see that our proposed CSPDSoS approach exhibits superior performance in estimating  $\Pi_r$  and  $\Pi_c$  when we increase  $n, L$ , or the overall sparsity  $\rho$ . This observation validates our theoretical findings. Additionally, it is noteworthy that CSPDSoS consistently outperforms CSPSoS, and both methods significantly surpass CSPSum, indicating the effectiveness of our proposed approach.

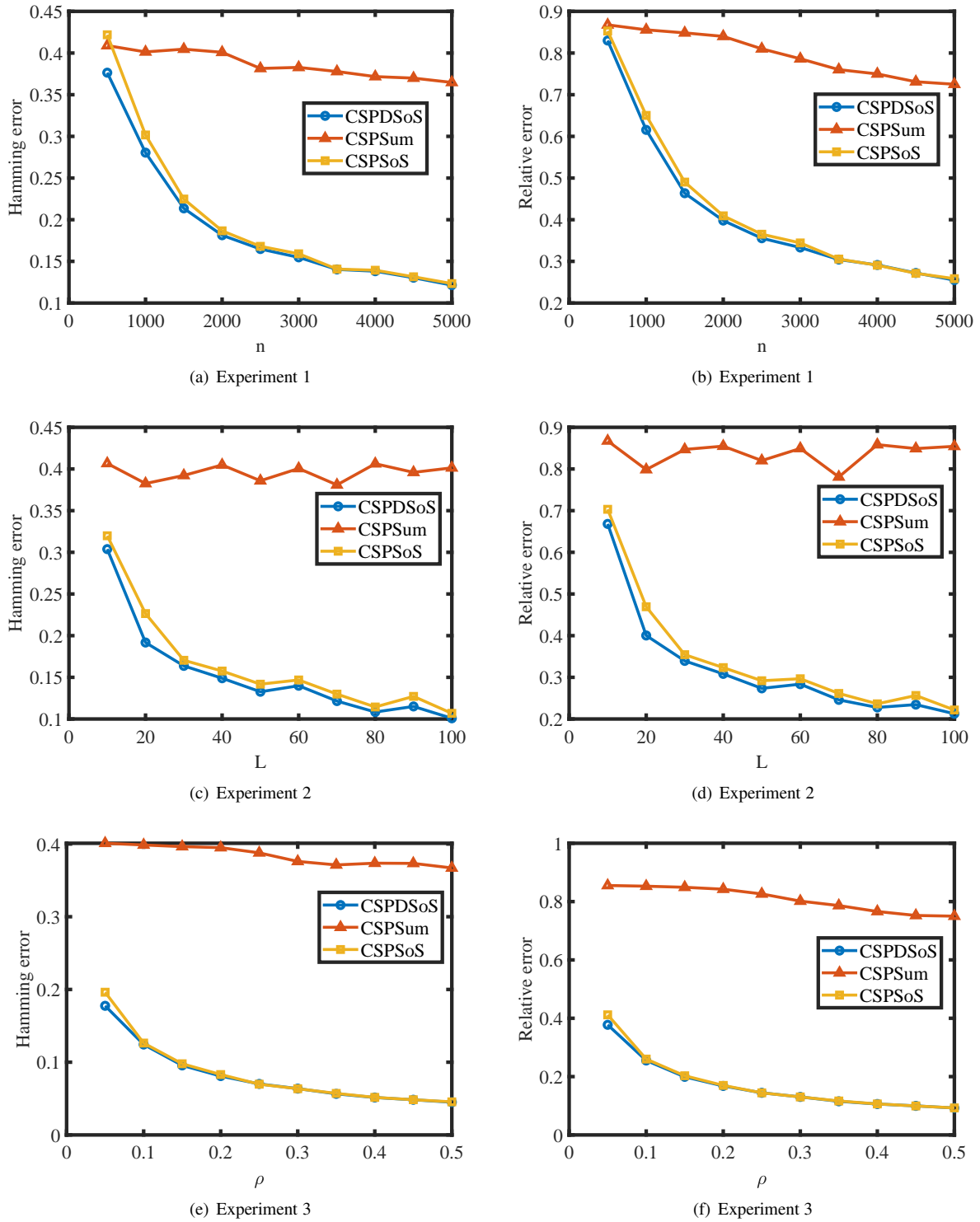


Figure 2: Numerical results of Experiments 1-3.

## 6.2. Real data

We apply our CSPDSoS to the FAO Multiplex Trade Network (FAOMTN), a real-world multi-layer directed network accessible for download at <https://manliodedomenico.com/data.php> in this subsection. This dataset constitutes a comprehensive global network of food imports and exports, featuring multiple layers that represent different products. The nodes in this network denote individual countries, while the edges within each layer represent the import/export connections between countries for a particular product. The dataset, compiled in 2010, encompasses 364 products and 213 countries [31], where we have consolidated China and China-mainland into a single category labeled “China” to ensure consistency. We have arranged the layers in decreasing order according to their total edge count and selected the 30 most densely connected layers (i.e.,  $n = 213, L = 30$ ). For a comprehensive listing of the 30 products utilized in this study, please refer to Table 1.

Initially, the data was weighted, but we have simplified it to an unweighted format whenever a trade relationship exists between countries. To enhance interpretability, we have set  $K = 6$ , representing the number of continents excluding Antarctica. For a country  $i$ , if  $\max_{k \in [K]} \hat{\Pi}_r(i, k) \leq 0.5$ , it is classified as a highly mixed export country, suggesting a diversified economy with exports to various countries. Similarly, if  $\max_{k \in [K]} \hat{\Pi}_c(i, k) \leq 0.5$ , it is deemed a highly mixed import country. Figure 3 shows the lists of these highly mixed export (import) countries and their estimated mixed memberships obtained from CSPDSoS. The term  $\text{argmax}_{k \in [K]} \hat{\Pi}_r(i, k)$  (and  $\text{argmax}_{k \in [K]} \hat{\Pi}_c(i, k)$ ) refers to the home base row (and column) community of node  $i$  for  $i \in [n]$ . Figure 4 presents the home base community assignments returned by the CSPDSoS method for three selected layers, offering a clear visualization of the identified communities. Figure 5 presents a visual representation of the estimated home base row and column communities for the 213 countries considered in this study. Notably, the structure of the row (export) communities exhibits distinct differences compared to the column (import) communities, indicating a variance in trade patterns across exporting and importing nations.

Table 1: List of products considered in this article.

“Soybeans”	“Food prep nes”	“Crude materials”	“Wine”	“Wheat”
“Oil, palm”	“Meat, cattle, boneless (beef & veal)”	“Cake, soybeans”	“Beverages, distilled alcoholic”	“Maize”
“Cheese, whole cow milk”	“Rubber natural dry”	“Cigarettes”	“Pastry”	“Chocolate products nes”
“Coffee, green”	“Meat, port”	“Meat, chicken”	“Sugar Raw Centrifugal”	“Cotton lint”
“Beverages, non alcoholic”	“Bananas”	“Rice, milled”	“Tobacco, unmanufactured”	“Fruit, prepared nes”
“Sugar refined”	“Beer of barley”	“Meat, pig”	“Cocoa, beans”	“Pet food”

## 7. Conclusion

This article contributes to the field of overlapping community detection in multi-layer directed networks by introducing both a novel model and an effective algorithm. The proposed multi-layer MM-ScBM model offers a novel framework that extends existing models to accommodate the complexities of multi-layer directed networks. The spectral procedure we have developed for estimating nodes’ memberships enjoys consistent estimation properties under the proposed model. Our theoretical analysis has revealed that factors such as increased sparsity, larger node sets, and more layers in the network can enhance the accuracy of overlapping community detection. Extensive numerical experiments have not only verified our theoretical claims but also highlighted the outstanding performance of our method when compared to its competitors. The application of our algorithm to a real-world multi-layer directed network has produced insightful results, highlighting the potential of our approach in uncovering meaningful overlapping community structures. In summary, our work offers powerful tools for the analysis of multi-layer directed networks.

Future works could focus on several directions to further advance the field of overlapping community detection in multi-layer directed networks. Firstly, extending the proposed multi-layer MM-ScBM model to accommodate dynamic changes in the network structure, such as the evolution of overlapping communities over time, would be a valuable contribution. Secondly, investigating the potential of incorporating additional network features, such as node attributes or edge weights, into the multi-layer MM-ScBM model could enhance its expressiveness and improve the accuracy of overlapping community detection. Thirdly, developing efficient methods to estimate the number of communities in multi-layer networks represents a challenging and promising direction. Lastly, accelerating the proposed spectral procedure would be crucial for handling large-scale multi-layer directed networks.

	$\hat{\Pi}_r$					
	Community 1	Community 2	Community 3	Community 4	Community 5	Community 6
Austria	0.1775	0.1661	0.2291	0.1981	0.2291	0
Belgium	0.1554	0.3049	0.1489	0.0789	0.3118	0
Denmark	0.1787	0.1493	0.2359	0.1538	0.2822	0
Finland	0.2103	0.1398	0.2164	0.1948	0.2387	0
Ireland	0.2145	0.1556	0.2193	0.1854	0.2252	0
Kazakhstan	0.1402	0.0896	0.2185	0.2414	0.3103	0
Poland	0.1655	0.1818	0.2339	0.1755	0.2433	0
Russia	0.2033	0.1182	0.2171	0.2125	0.249	0
Spain	0.2228	0.1477	0.1402	0.2963	0.1931	0
Sweden	0.2128	0.1424	0.2244	0.1933	0.2271	0
Switzerland	0.1702	0.089	0.1703	0.1509	0.2163	0.2033
Turkey	0.1118	0.0854	0.1215	0.1408	0.1511	0.3894
Ukraine	0.2027	0.1138	0.2162	0.2187	0.2486	0
United Kingdom	0.1597	0	0.2357	0.1531	0.335	0.1166
Bahamas	0.1585	0.123	0.1097	0.1217	0.1659	0.3211
Bosnia and Herzegovina	0.193	0.1605	0.2258	0.1919	0.2288	0
Bulgaria	0.2053	0.1236	0.2248	0.2209	0.2254	0
Croatia	0.1974	0.1494	0.2248	0.1956	0.2328	0
Cyprus	0.2143	0.1393	0.2225	0.2085	0.2154	0
Czech Republic	0.2014	0.1487	0.2354	0.1867	0.2277	0
Greece	0.1963	0.1456	0.2263	0.225	0.2067	0
Hungary	0.1971	0.1271	0.2186	0.2107	0.2465	0
Israel	0.147	0.1243	0.1444	0.132	0.1739	0.2764
Lithuania	0.1953	0.1267	0.2281	0.1969	0.2531	0
Luxembourg	0.2185	0.127	0.2323	0.193	0.2291	0
Montenegro	0.1964	0.1427	0.2454	0.1931	0.2224	0
Norway	0.1704	0.1332	0.1494	0.1414	0.1941	0.2113
Portugal	0.2135	0.1472	0.2089	0.1956	0.2347	0
Republic of Moldova	0.2227	0.1047	0.2169	0.221	0.2346	0
Romania	0.1948	0.1273	0.2242	0.2057	0.248	0
Serbia	0.2104	0.1265	0.2331	0.1981	0.2319	0
Slovakia	0.2207	0.1388	0.2238	0.1982	0.2185	0
Slovenia	0.2101	0.1455	0.223	0.196	0.2254	0
The former Yugoslav Republic of Macedonia	0.2061	0.1523	0.2292	0.2012	0.2112	0
Unspecified	0.1496	0.1055	0.1873	0.205	0.2048	0.1479
Chile	0.1014	0.0376	0.0771	0.1501	0.1479	0.4858
Estonia	0.1983	0.1519	0.2249	0.1999	0.225	0
Georgia	0.2042	0.1426	0.2114	0.206	0.2359	0
Armenia	0.1875	0.1408	0.2416	0.1926	0.2375	0
Belarus	0.2169	0.1489	0.2281	0.192	0.2141	0
Latvia	0.205	0.1424	0.2241	0.1966	0.232	0
Azerbaijan	0.1999	0.1716	0.1573	0.1476	0.206	0.1176
Bermuda	0.2141	0.1084	0.2059	0.2	0.2717	0
Malta	0.1425	0.1057	0.1113	0.1588	0.193	0.2886
Greenland	0.1066	0.0701	0.0951	0.0851	0.153	0.4901

	$\hat{\Pi}_c$					
	Community 1	Community 2	Community 3	Community 4	Community 5	Community 6
Australia	0.0242	0.0618	0.3073	0.3518	0	0.2548
Belgium	0	0	0.2873	0.3053	0.4074	0
Italy	0	0	0.2355	0.3034	0.461	0
Japan	0.0556	0.0585	0.2745	0.3168	0	0.2946
Netherlands	0	0	0.2902	0.357	0.3527	0
Korea, Republic of	0.0212	0.0246	0.2495	0.2549	0	0.4498
Singapore	0.0498	0.009	0.243	0.2435	0	0.4547
Spain	0.0053	0.0056	0.2287	0.2606	0.4998	0
Sweden	0.0208	0.0393	0.2103	0.2378	0.4626	0.0292
Switzerland	0	0.0043	0.2971	0.3035	0.3952	0
Turkey	0.0253	0.0168	0.1096	0.1265	0.3285	0.3932
United Kingdom	0.0259	0	0.3054	0.3618	0.3069	0
Albania	0	0.012	0	0	0.4967	0.4913
Cyprus	0.0134	0.0356	0	0.01	0.4507	0.4902
Israel	0.0001	0.0391	0.1157	0.1502	0.2502	0.4446
Luxembourg	0.0107	0.0278	0	0	0.4932	0.4683
Norway	0.0359	0.0274	0.2118	0.2314	0.3219	0.1716
Portugal	0.0219	0.0137	0.0744	0.1106	0.4378	0.3416
Republic of Moldova	0.0039	0.0122	0	0	0.491	0.4928
New Zealand	0.0312	0.022	0.2263	0.2429	0	0.4776

(b) Heatmap of the estimated mixed memberships for highly mixed import countries.

Figure 3: Estimated memberships of highly mixed countries.

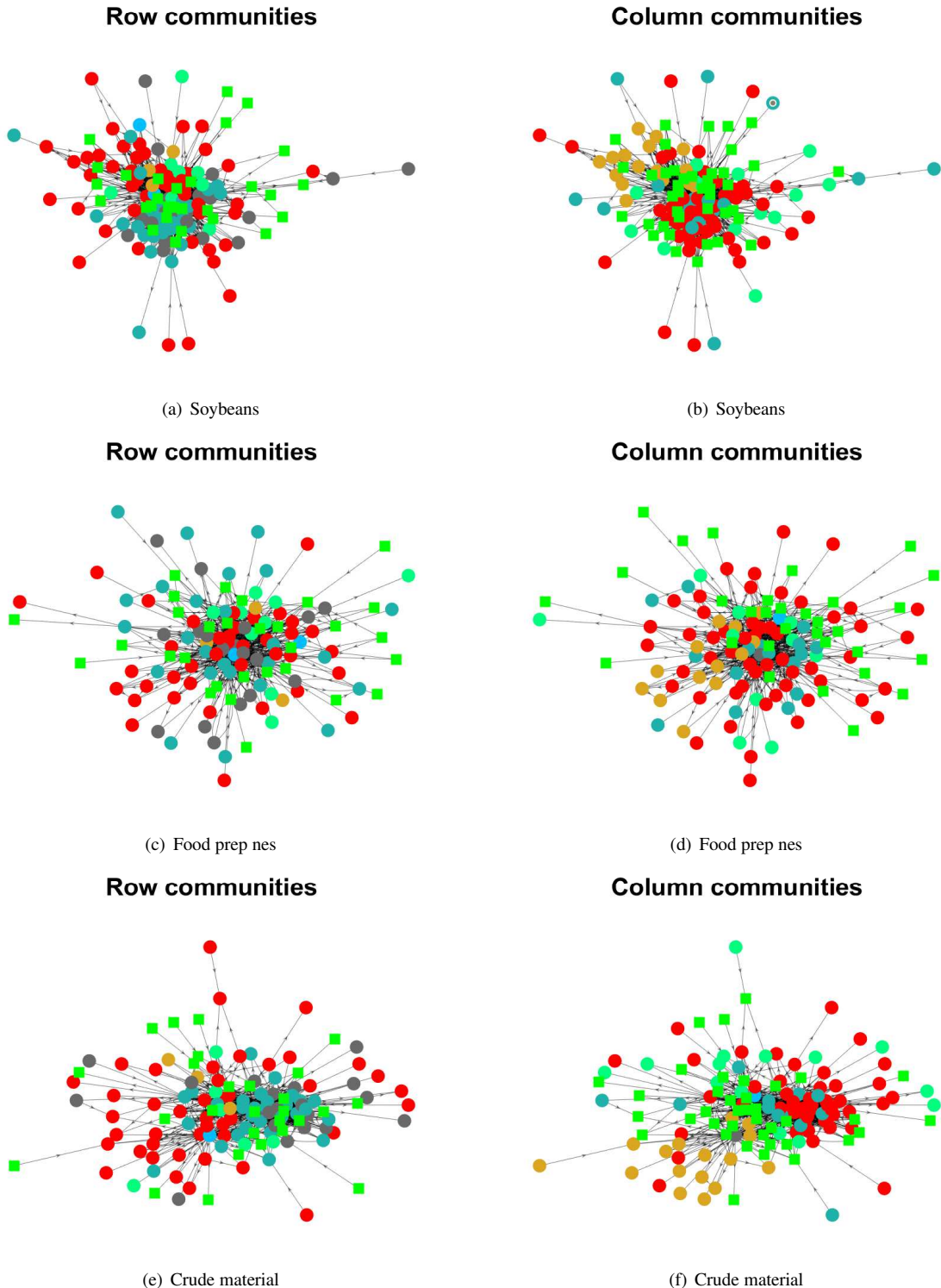


Figure 4: Examples of the home base community assignments for the three layers: Soybeans, Food prep nes, and Crude material. Colors indicate communities and green squares mean highly mixed nodes. For visualization, we do not show isolated nodes for the three layers.

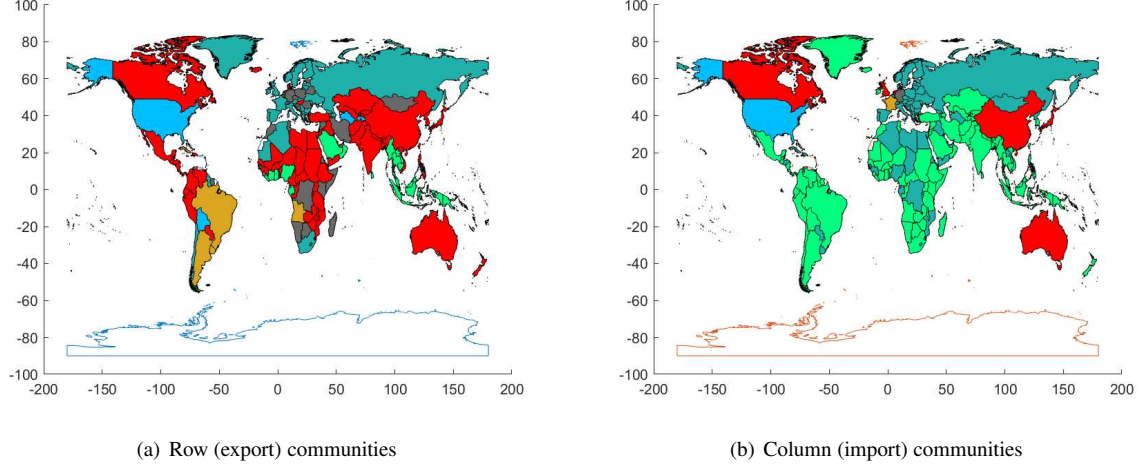


Figure 5: Row (export) and column (import) communities discovered by CSPDSoS for FAOMTN. Colors represent communities.

### CRediT authorship contribution statement

**Huan Qing:** Conceptualization, Data curation, Formal analysis, Funding acquisition, Investigation, Methodology, Project administration, Resources, Software, Supervision, Validation, Visualization, Writing – original draft, Writing - review & editing.

### Declaration of competing interest

The author declares no competing interests.

### Data availability

Data and code will be made available on request.

### Acknowledgements

Qing's work was sponsored by the Scientific Research Foundation of Chongqing University of Technology (Grant No: 0102240003) and the Natural Science Foundation of Chongqing, China (Grant No: CSTB2023NSCQ-LZX0048).

### Appendix A. Proofs of theoretical results

#### Appendix A.1. Proof of Lemma 1.

*Proof.* By the pure node condition,  $\text{rank}(\Pi_r) = K$  and  $\text{rank}(\Pi_c) = K$ . Since  $\tilde{S}_r = \Pi_r(\rho^2 \sum_{l \in [L]} B_l \Pi'_c \Pi_c B'_l) \Pi'_r$ , we have  $\text{rank}(\tilde{S}_r) = \text{rank}(\sum_{l \in [L]} B_l B'_l)$ . Therefore, when  $\text{rank}(\sum_{l \in [L]} B_l B'_l) = K$ , the rank of  $\tilde{S}_r$  is  $K$ , i.e.,  $\tilde{S}_r$  is a low rank matrix with only  $K$  nonzero eigenvalues. Let  $\tilde{S}_r = U_r \Lambda_r U'_r$  be the leading  $K$  eigendecomposition of  $\tilde{S}_r$ . Thus,  $U_r \Lambda_r U'_r = \Pi_r(\rho^2 \sum_{l \in [L]} B_l \Pi'_c \Pi_c B'_l) \Pi'_r$ , which gives that  $U_r = \Pi_r(\rho^2 \sum_{l \in [L]} B_l \Pi'_c \Pi_c B'_l) \Pi'_r U_r \Lambda_r^{-1}$ . Setting  $X_r = (\rho^2 \sum_{l \in [L]} B_l \Pi'_c \Pi_c B'_l) \Pi'_r U_r \Lambda_r^{-1}$  gives  $U_r = \Pi_r X_r$ . Since  $U_r(\mathcal{I}_r, :) = (\Pi_r X_r)(\mathcal{I}_r, :) = \Pi_r(\mathcal{I}_r, :) X_r = X_r$ , we have  $X_r = U_r(\mathcal{I}_r, :)$ , i.e.,  $U_r = \Pi_r U_r(\mathcal{I}_r, :)$ . Similarly,  $U_c = \Pi_c U_c(\mathcal{I}_c, :)$ .  $\square$

### Appendix A.2. Proof of Theorem 1

*Proof.* First, we have the following lemma.

**Lemma 2.** *When Assumption 1 holds, with probability  $1 - o(\frac{1}{n+L})$ ,*

$$\|S_r - \tilde{S}_r\|_\infty = O(\sqrt{\rho^2 n^2 L \log(n+L)}) + O(\rho^2 n L), \|S_c - \tilde{S}_c\|_\infty = O(\sqrt{\rho^2 n^2 L \log(n+L)}) + O(\rho^2 n L).$$

*Proof.* For  $\|S_r - \tilde{S}_r\|_\infty$ , we have

$$\begin{aligned} \|S_r - \tilde{S}_r\|_\infty &= \max_{i \in [n]} \left( \sum_{j \neq i, j \in [n]} \left| \sum_{l \in [L]} \sum_{m \in [n]} (A_l(i, m) A_l(j, m) - \Omega_l(i, m) \Omega_l(j, m)) \right| + \sum_{l \in [L]} \sum_{m \in [n]} \Omega_l^2(i, m) \right) \\ &\leq \max_{i \in [n]} \left( \sum_{j \neq i, j \in [n]} \left| \sum_{l \in [L]} \sum_{m \in [n]} (A_l(i, m) A_l(j, m) - \Omega_l(i, m) \Omega_l(j, m)) \right| + \sum_{l \in [L]} \sum_{m \in [n]} \rho^2 \right) \\ &= \max_{i \in [n]} \left( \sum_{j \neq i, j \in [n]} \left| \sum_{l \in [L]} \sum_{m \in [n]} (A_l(i, m) A_l(j, m) - \Omega_l(i, m) \Omega_l(j, m)) \right| + \rho^2 n L. \right) \end{aligned}$$

Let  $x$  be any vector in  $\mathbb{R}^{(n-1) \times 1}$ ,  $y_{(i,j)} = \sum_{l \in [L]} \sum_{m \in [n]} (A_l(i, m) A_l(j, m) - \Omega_l(i, m) \Omega_l(j, m))$  for  $i \in [n], j \neq i, j \in [n]$ , and  $T_{(i)} = \sum_{j \neq i, j \in [n]} y_{(i,j)} x(j)$  for  $i \in [n]$ . Set  $\tau = \max(\max_{i \in [n]} \max_{j \in [n]} |\sum_{l \in [L]} \sum_{m \in [n]} (A_l(i, m) A_l(j, m) - \Omega_l(i, m) \Omega_l(j, m))|, \max_{i \in [n]} \max_{j \in [n]} |\sum_{l \in [L]} \sum_{m \in [n]} (A_l(m, i) A_l(m, j) - \Omega_l(m, i) \Omega_l(m, j))|)$ . For  $i \in [n], j \neq i, j \in [n]$ , we have  $\mathbb{E}(y_{(i,j)} x(j)) = 0$  since  $j \neq i$ ,  $|y_{(i,j)} x(j)| \leq \tau \|x\|_\infty$ , and

$$\begin{aligned} \sum_{j \neq i, j \in [n]} \mathbb{E}[y_{(i,j)}^2 x^2(j)] &= \sum_{j \neq i, j \in [n]} x^2(j) \mathbb{E}[y_{(i,j)}^2] = \sum_{j \neq i, j \in [n]} x^2(j) \sum_{l \in [L]} \sum_{m \in [n]} \Omega_l(i, m) \Omega_l(j, m) (1 - \Omega_l(i, m) \Omega_l(j, m)) \\ &\leq \sum_{j \neq i, j \in [n]} x^2(j) \sum_{l \in [L]} \sum_{m \in [n]} \Omega_l(i, m) \Omega_l(j, m) \leq \sum_{j \neq i, j \in [n]} x^2(j) \sum_{l \in [L]} \sum_{m \in [n]} \rho^2 = \rho^2 \|x\|_F^2 n L. \end{aligned}$$

By Theorem 1.4 (Bernstein inequality) of [22], let  $t$  be any nonnegative value, we have

$$\mathbb{P}(|T_{(i)}| \geq t) \leq \exp\left(\frac{-t^2/2}{\rho^2 \|x\|_F^2 n L + \frac{\tau \|x\|_\infty t}{3}}\right).$$

Let  $t$  be  $\sqrt{\rho^2 \|x\|_F^2 n L \log(n+L)} \times \frac{\alpha+1+\sqrt{(\alpha+1)(\alpha+19)}}{3}$  for any  $\alpha \geq 0$ . When  $\rho^2 \|x\|_F^2 n L \geq \tau^2 \|x\|_\infty^2 \log(n+L)$  holds, the following inequality holds:

$$\mathbb{P}(|T_{(i)}| \geq t) \leq \exp(-(\alpha+1) \log(n+L) \frac{1}{\frac{18}{(\sqrt{\alpha+1} + \sqrt{\alpha+19})^2} + \frac{2\sqrt{\alpha+1}}{\sqrt{\alpha+1} + \sqrt{\alpha+19}} \sqrt{\frac{\tau^2 \|x\|_\infty^2 \log(n+L)}{\rho^2 \|x\|_F^2 n L}}}) \leq \frac{1}{(n+L)^{\alpha+1}}.$$

Since  $x$  can be any  $(n-1) \times 1$  vector and  $\alpha$  is any nonnegative value, letting  $x$ 's elements be in  $\{-1, 1\}$  and  $\alpha = 1$  gives: when  $\rho^2 n^2 L \geq \tau^2 \log(n+L)$ , with probability  $1 - o(\frac{1}{n+L})$ ,

$$\max_{i \in [n]} |T_{(i)}| = O(\sqrt{\rho^2 n^2 L \log(n+L)}),$$

which gives  $\|S_r - \tilde{S}_r\|_\infty = O(\sqrt{\rho^2 n^2 L \log(n+L)}) + O(\rho^2 n L)$ . Similarly,  $\|S_c - \tilde{S}_c\|_\infty = O(\sqrt{\rho^2 n^2 L \log(n+L)}) + O(\rho^2 n L)$ . For simplicity, we restrict our consideration to the highly sparse regime  $\tau \leq c_3$  for some constant  $c_3 > 0$ . For this sparse regime, the requirement  $\rho^2 n^2 L \geq \tau^2 \log(n+L)$  reduces to Assumption 1.  $\square$

According to Theorem 4.2 [23], when  $|\lambda_K(\tilde{S}_r)| \geq 4\|S_r - \tilde{S}_r\|_\infty$  and  $|\lambda_K(\tilde{S}_c)| \geq 4\|S_c - \tilde{S}_c\|_\infty$  hold, there are two orthogonal matrices  $O_r$  and  $O_c$  such that

$$\|\hat{U}_r - U_r O_r\|_{2 \rightarrow \infty} \leq 14 \frac{\|S_r - \tilde{S}_r\|_\infty \|U_r\|_{2 \rightarrow \infty}}{|\lambda_K(\tilde{S}_r)|}, \|\hat{U}_c - U_c O_c\|_{2 \rightarrow \infty} \leq 14 \frac{\|S_c - \tilde{S}_c\|_\infty \|U_c\|_{2 \rightarrow \infty}}{|\lambda_K(\tilde{S}_c)|}.$$

Because  $\varpi_r := \|\hat{U}_r \hat{U}'_r - U_r U'_r\|_{2 \rightarrow \infty} \leq 2\|\hat{U}_r - U_r O_r\|_{2 \rightarrow \infty}$  and  $\varpi_c := \|\hat{U}_c \hat{U}'_c - U_c U'_c\|_{2 \rightarrow \infty} \leq 2\|\hat{U}_c - U_c O_c\|_{2 \rightarrow \infty}$ , we have

$$\varpi_r \leq 28 \frac{\|S_r - \tilde{S}_r\|_\infty \|U_r\|_{2 \rightarrow \infty}}{|\lambda_K(\tilde{S}_r)|}, \varpi_c \leq 28 \frac{\|S_c - \tilde{S}_c\|_\infty \|U_c\|_{2 \rightarrow \infty}}{|\lambda_K(\tilde{S}_c)|}.$$

Based on Lemma 3.1 [17] and Condition 1, we have  $\|U_r\|_{2 \rightarrow \infty} = O(\sqrt{\frac{1}{n}})$  and  $\|U_c\|_{2 \rightarrow \infty} = O(\sqrt{\frac{1}{n}})$ , which give that

$$\varpi_r = O\left(\frac{\|S_r - \tilde{S}_r\|_\infty}{|\lambda_K(\tilde{S}_r)| \sqrt{n}}\right), \varpi_c = O\left(\frac{\|S_c - \tilde{S}_c\|_\infty}{|\lambda_K(\tilde{S}_c)| \sqrt{n}}\right).$$

Combining Assumption 2 and Condition 1 gives the following result:

$$\begin{aligned} |\lambda_K(\tilde{S}_r)| &= \sqrt{\lambda_K\left(\left(\sum_{l \in [L]} \Omega_l \Omega'_l\right)^2\right)} = \sqrt{\lambda_K\left(\left(\sum_{l \in [L]} \rho^2 \Pi_r B_l \Pi'_c \Pi_c B'_l \Pi'_r\right)^2\right)} = \rho^2 \sqrt{\lambda_K^2\left(\sum_{l \in [L]} \Pi_r B_l \Pi'_c \Pi_c B'_l \Pi'_r\right)} \\ &= \rho^2 \sqrt{\lambda_K^2\left(\Pi_r \left(\sum_{l \in [L]} B_l \Pi'_c \Pi_c B'_l\right) \Pi'_r\right)} = \rho^2 \sqrt{\lambda_K^2\left(\Pi'_r \Pi_r \left(\sum_{l \in [L]} B_l \Pi'_c \Pi_c B'_l\right)\right)} \geq \rho^2 \lambda_K(\Pi'_r \Pi_r) \sqrt{\lambda_K^2\left(\sum_{l \in [L]} B_l \Pi'_c \Pi_c B'_l\right)} \\ &= O(\rho^2 \lambda_K(\Pi'_r \Pi_r) \lambda_K(\Pi'_c \Pi_c) |\lambda_K(\sum_{l \in [L]} B_l B'_l)|) = O(\rho^2 n^2 L). \end{aligned}$$

Similarly, we have  $|\lambda_K(\tilde{S}_c)| \geq O(\rho^2 n^2 L)$ . Therefore, we have

$$\varpi_r = O\left(\frac{\|S_r - \tilde{S}_r\|_\infty}{\rho^2 n^{2.5} L}\right), \varpi_c = O\left(\frac{\|S_c - \tilde{S}_c\|_\infty}{\rho^2 n^{2.5} L}\right).$$

By the proof of Theorem 3.2 of [17], we have

$$\begin{aligned} \max_{i \in [n]} \|e'_i(\hat{\Pi}_r - \Pi_r \mathcal{P}_r)\|_1 &= O(\varpi_r \kappa(\Pi'_r \Pi_r) \sqrt{\lambda_1(\Pi'_r \Pi_r)}) = O(\varpi_r \sqrt{\frac{n}{K}}) = O(\varpi_r \sqrt{n}) = O\left(\frac{\|S_r - \tilde{S}_r\|_\infty}{\rho^2 n^2 L}\right), \\ \max_{i \in [n]} \|e'_i(\hat{\Pi}_c - \Pi_c \mathcal{P}_c)\|_1 &= O(\varpi_c \kappa(\Pi'_c \Pi_c) \sqrt{\lambda_1(\Pi'_c \Pi_c)}) = O(\varpi_c \sqrt{\frac{n}{K}}) = O(\varpi_c \sqrt{n}) = O\left(\frac{\|S_c - \tilde{S}_c\|_\infty}{\rho^2 n^2 L}\right), \end{aligned}$$

where  $\mathcal{P}_r$  and  $\mathcal{P}_c$  are two  $K \times K$  permutation matrices. By Lemma 2, this theorem holds.  $\square$

## References

- [1] W. Su, X. Guo, X. Chang, Y. Yang, Spectral co-clustering in multi-layer directed networks, Computational Statistics & Data Analysis (2024) 107987.
- [2] S. Fortunato, Community detection in graphs, Physics Reports 486 (3-5) (2010) 75–174.
- [3] S. Fortunato, D. Hric, Community detection in networks: A user guide, Physics Reports 659 (2016) 1–44.
- [4] Q. Han, K. Xu, E. Airoldi, Consistent estimation of dynamic and multi-layer block models, in: International Conference on Machine Learning, PMLR, 2015, pp. 1511–1520.
- [5] S. Paul, Y. Chen, Spectral and matrix factorization methods for consistent community detection in multi-layer networks, Annals of Statistics 48 (1) (2020) 230 – 250.
- [6] J. Lei, K. Chen, B. Lynch, Consistent community detection in multi-layer network data, Biometrika 107 (1) (2020) 61–73.
- [7] J. Lei, K. Z. Lin, Bias-adjusted spectral clustering in multi-layer stochastic block models, Journal of the American Statistical Association 118 (544) (2023) 2433–2445.
- [8] P. W. Holland, K. B. Laskey, S. Leinhardt, Stochastic blockmodels: First steps, Social Networks 5 (2) (1983) 109–137.
- [9] B.-Y. Jing, T. Li, Z. Lyu, D. Xia, Community detection on mixture multilayer networks via regularized tensor decomposition, Annals of Statistics 49 (6) (2021) 3181–3205.
- [10] J. Arroyo, A. Athreya, J. Cape, G. Chen, C. E. Priebe, J. T. Vogelstein, Inference for multiple heterogeneous networks with a common invariant subspace, Journal of Machine Learning Research 22 (142) (2021) 1–49.
- [11] X. Fan, M. Pensky, F. Yu, T. Zhang, Alma: Alternating minimization algorithm for clustering mixture multilayer network, Journal of Machine Learning Research 23 (330) (2022) 1–46.
- [12] S. Xu, Y. Zhen, J. Wang, Covariate-assisted community detection in multi-layer networks, Journal of Business & Economic Statistics 41 (3) (2023) 915–926.

- [13] K. Rohe, T. Qin, B. Yu, Co-clustering directed graphs to discover asymmetries and directional communities, *Proceedings of the National Academy of Sciences* 113 (45) (2016) 12679–12684.
- [14] N. Gillis, S. A. Vavasis, Fast and robust recursive algorithms for separable nonnegative matrix factorization, *IEEE Transactions on Pattern Analysis and Machine Intelligence* 36 (4) (2013) 698–714.
- [15] E. M. Airoldi, D. M. Blei, S. E. Fienberg, E. P. Xing, Mixed membership stochastic blockmodels, *Journal of Machine Learning Research* 9 (2008) 1981–2014.
- [16] E. M. Airoldi, X. Wang, X. Lin, Multi-way blockmodels for analyzing coordinated high-dimensional responses, *Annals of Applied Statistics* 7 (4) (2013) 2431.
- [17] X. Mao, P. Sarkar, D. Chakrabarti, Estimating mixed memberships with sharp eigenvector deviations, *Journal of the American Statistical Association* 116 (536) (2021) 1928–1940.
- [18] J. Jin, Z. T. Ke, S. Luo, Mixed membership estimation for social networks, *Journal of Econometrics* 239 (2) (2024) 105369.
- [19] H. Qing, J. Wang, Regularized spectral clustering under the mixed membership stochastic block model, *Neurocomputing* 550 (2023) 126490.
- [20] M. C. U. Araújo, T. C. B. Saldanha, R. K. H. Galvao, T. Yoneyama, H. C. Chame, V. Visani, The successive projections algorithm for variable selection in spectroscopic multicomponent analysis, *Chemometrics and Intelligent Laboratory Systems* 57 (2) (2001) 65–73.
- [21] N. Gillis, S. A. Vavasis, Semidefinite programming based preconditioning for more robust near-separable nonnegative matrix factorization, *SIAM Journal on Optimization* 25 (1) (2015) 677–698.
- [22] J. A. Tropp, User-friendly tail bounds for sums of random matrices, *Foundations of computational mathematics* 12 (2012) 389–434.
- [23] J. Cape, M. Tang, C. E. Priebe, The two-to-infinity norm and singular subspace geometry with applications to high-dimensional statistics, *Annals of Statistics* 47 (5) (2019) 2405–2439.
- [24] J. Lei, A. Rinaldo, Consistency of spectral clustering in stochastic block models, *Annals of Statistics* 43 (1) (2015) 215–237.
- [25] M. Panov, K. Slavnov, R. Ushakov, Consistent estimation of mixed memberships with successive projections, in: *Complex Networks & Their Applications VI: Proceedings of Complex Networks 2017 (The Sixth International Conference on Complex Networks and Their Applications)*, Springer, 2018, pp. 53–64.
- [26] H. Qing, J. Wang, Bipartite mixed membership distribution-free model. a novel model for community detection in overlapping bipartite weighted networks, *Expert Systems with Applications* 235 (2024) 121088.
- [27] O. Klopp, M. Panov, S. Sigalla, A. B. Tsybakov, Assigning topics to documents by successive projections, *The Annals of Statistics* 51 (5) (2023) 1989–2014.
- [28] Z. T. Ke, M. Wang, Using svd for topic modeling, *Journal of the American Statistical Association* 119 (545) (2024) 434–449.
- [29] H. Qing, Finding mixed memberships in categorical data, *Information Sciences* (2024) 120785.
- [30] L. Chen, Y. Gu, A spectral method for identifiable grade of membership analysis with binary responses, *Psychometrika* (2024) 1–32.
- [31] M. De Domenico, V. Nicosia, A. Arenas, V. Latora, Structural reducibility of multilayer networks, *Nature Communications* 6 (1) (2015) 6864.